J. Biochem. 121, 746-755 (1997)

Measurement of the Membrane Potential Generated by Complex I in Submitochondrial Particles

Anna Ghelli,* Bruna Benelli,* and Mauro Degli Esposti†,[1]

*Department of Biology, University of Bologna, Italy; and †Department of Biochemistry and Molecular Biology, Monash University, Wellington Road, Clayton, 3168 Victoria, Australia

Received for publication, December 9, 1996

To investigate the energy-conserving function of the NADH:ubiquinone reductase (complex I), we have selected oxonol VI [bis(3-propyl-5-oxoisoxazol-4-yl)pentamethine oxonol] as the most sensitive probe for measuring the reactions of membrane potential generation in submitochondrial particles. Calibration of the oxonol signals with potassium diffusion potentials shows a non-linear response after a threshold around −50 mV. Thermodynamic evaluations indicate that the upper limit of the oxonol response to the potential generated by complex I is around −220 mV, which is close to the maximal protonmotive force in coupled submitochondrial particles. NADH addition to particles in which ubiquinol oxidation is blocked by inhibitors of other respiratory complexes generates oxonol signals corresponding to membrane potentials of −130 to −180 mV. These signals are produced by about four turnovers of the complex reducing endogenous ubiquinone (*i.e.* non-steady-state conditions) and are equivalent to a charge separation similar to that of the antimycin-sensitive reactions of ubiquinol:cytochrome *c* reductase (complex III). The transient oxonol signals under non-steady-state conditions are thus informative of crucial steps in the electrogenic reactions catalyzed by complex I. The possible nature of these electrogenic reactions is discussed in relation to proposed mechanisms for complex I.

Key words: membrane potential, mitochondria, NADH:ubiquinone reductase, ubiquinone.

NADH:ubiquinone (Q) reductase (EC 1.6.99.3, also known as complex I) constitutes the first phosphorylation site in the respiratory chain of mitochondria (*1, 2*) and several bacteria (*3*). Complex I remains the least known among the respiratory complexes of mitochondria, not only for its intricate structure, but also for the uncertainties regarding its catalytic mechanism (*1, 2*). These uncertainties derive in part from the lack of sensitive techniques to measure the bioenergetic functions of complex I. Along our studies on the mechanism of proton and electron transport of complex I (*4*), we have examined various methods for measuring the electric membrane potential generated by the NADH:Q reductase activity in coupled submitochondrial particles.

Whilst cationic dyes such as safranine-O have been used in mitochondria (*5, 6*), anionic dyes such as oxonol VI [bis(3-propyl-5-oxoisoxazol-4-yl)pentamethine oxonol] have been used in submitochondrial particles (*7-10*) or bacterial systems (*11*) to monitor the membrane potential generated by the NADH:Q reductase activity. Oxonol VI undergoes a large red-shift in its absorbance spectrum upon charging the membrane positively inside in closed membrane systems, and optical signals around 0.04-0.1 *A* have been reported for NADH-respiring submitochondrial particles (*7, 8, 12, 13*). In earlier studies we focused on specific applications, *viz.* quinone specificity (*12*) of steady-state measurements with oxonol VI. The purpose of this work is to demonstrate the usefulness of the oxonol assay in the study of the bioenergetic function of complex I within the native mitochondrial membrane. The novelity of the work is the demonstration of how oxonol enables sensitive measurements of non-steady-state processes in the proton and electron transport from NADH to ubiquinone.

MATERIALS AND METHODS

Preparations—Phosphorylating submitochondrial particles (ETP_H) were prepared from bovine heart mitochondria as described by Hansen and Smith (*14*). The particles were stored at −70°C at 40-50 mg/ml [protein was measured by biuret method (*12, 14*) in 0.25 M sucrose and 20 mM tricine-OH, pH 7.6, containing 5 mM $MgCl_2$, 2 mM K-ATP, 2 mM K-succinate, and 2 mM reduced glutathione (*14, 15*)].

Reagents—2,3-Dimethoxy-5-methyl-6-*n*-undecylbenzoquinone (undecyl-Q or UBQ) was kindly provided by E. Berry, University of California, Berkeley, CA, USA, and decyl-Q (DB) was purchased from Sigma, St. Louis. Reduced Q analogs were prepared as described earlier (*13*). The Q analogs were dissolved in ethanol and determined as described previously (*12*). The indicators diO-C_5-(3) and

[1] To whom correspondence should be addressed. Phone: +61 3 99051431, Fax: +61 3 99054699, E-mail: mauro.esposti@med.monash.edu.au

Abbreviations: CCCP, carbonyl cyanide *m*-chlorophenylhydrazone; DB, decyl analog of ubiquinone; DBH_2, reduced decyl-Q; EPR, electron paramagnetic resonance; ETP_H, electron transport submitochondrial particles; FCCP, carbonyl cyanide *p*-trifluoromethoxyphenylhydrazone; I_{50}, concentration yielding 50% of inhibition; mA, milliabsorbance; MOA, methoxyacrylate; Q, ubiquinone; UBQ, undecyl analog of ubiquinone; $UBQH_2$, reduced undecyl analog of ubiquinone.

oxonol VI were purchased from Molecular Probes, Eugene, OR, USA. Oxonol was determined in methanol with a molar absorption coefficient of 123 $mM^{-1} \cdot cm^{-1}$ at 600 nm. Rolliniastatin-1 and -2 were generously provided by Prof. D. Cortes, University of Valencia, Spain (*16*). Methoxyacrylate (MOA)-stilbene was kindly given by Dr. P. Rich, Bodmin Research Institute, Cornwall, UK. Carboxin was a gift of Dr. J. Hargreaves, AFRC, Long Ashton, UK. All other reagents were obtained from Sigma, St. Louis, USA. The concentration of inhibitors was determined spectrophotometrically (*16*).

Enzyme and Membrane Potential Assays—NADH:Q reductase activity was assayed with 100-150 μM NADH at 350-410 nm with an extinction coefficient of 5.5 $mM^{-1} \cdot cm^{-1}$ (*12, 16*). The electrical membrane potential generated by NADH oxidation of ETP_H was measured by using either safranine (*5, 17*) or oxonol VI (*7-9, 12, 18*). ETP_H from different sources were diluted in sucrose 0.125 M, tricine-OH 50 mM (pH 8.0) containing 2.5 mM $MgCl_2$ and 40 mM KCl (sucrose-tricine buffer) to 10 mg/ml protein and treated with 2 μg/mg oligomycin, 1 nmol/mg antimycin A, and 3 nmol/mg MOA-stilbene (*4, 12*). The absorption changes of safranine were routinely measured at 511-541 nm and those of oxonol VI at 630-601 nm with a dual-wavelength SIGMA-ZWII spectrophotometer at room temperature (22-25°C). The instrument was equipped with a rapid mixing apparatus completing mixing in approximately 0.1 s. The concentration range of the dyes was 16-20 and 1-4 μM for safranine and oxonol VI, respectively, whereas the submitochondrial particles were used at final protein concentrations of 0.1-1 mg/ml.

In some experiments we have followed the optical changes of cytochrome *b* at 563-575 nm after succinate reduction in the presence of antimycin A and MOA-stilbene. Under such conditions, the oxidation of the high-potential *b* haem by the protonmotive force (*17*) was measured using NADH to energize the particles. Because cytochrome *b* is a chromophore internal to the mitochondrial membrane, its oxidation promoted by NADH (which is a reducing substrate) in the presence of complex III inhibitors indicates an electron re-distribution between of the two *b*-haems due to charge separation across the membrane (*17*).

Calibration of the Oxonol Signals—The calibration of the optical signals of oxonol VI with the membrane potential was obtained with two different approaches. The first approach is the classical diffusion potential of potassium imposed in the presence of valinomycin (*9, 18-20*). ETP_H were diluted to 0.15 mg/ml in sucrose 0.125 mM, tricine-tris 50 mM pH 8.0 containing KCl 1 mM and treated with 1 μM valinomycin to render the membrane fully permeable to potassium. Potassium gradients were imposed by adding various concentrations of KCl under a constant ionic strength maintained by additions of choline-Cl. The $\Delta\psi$ values derived by imposed KCl gradients were calculated using the Nernst equilibrium equation (*19*). Because of the problem of the slow membrane permeability by oxonol (*9*), diffusion potentials were imposed within 30 s after the addition of oxonol to the particles.

The second approach consisted of a thermodynamic manipulation of the NADH:Q reductase activity by changing the ambient redox potential with different ratios of the donor couple NAD^+/NADH and of the acceptor couple DB/DBH_2. This approach is in principle similar to previous thermodynamic evaluations (*7, 17, 20, 21*). ETP_H treated as described above were diluted to 0.15 mg/ml in sucrose-tricine buffer containing 0.5 μM nigericin, 3 μM oxonol VI, and 25 μM carboxin and equilibrated at 25°C with different concentrations of NAD^+ before the addition of a fixed concentration of 100 μM NADH. (The concentrations of NADH and NAD^+ ensued saturation of the DB reductase activity of complex I with minimal effects of substrate or product inhibition.) Once the signal due to NADH oxidation returned to the baseline value, the reductase reaction was initiated by the addition of 30 μM DB and the maximal extent of the oxonol signal recorded. This generally occurred 3 s after the start of the reaction, when the concentration of DBH_2 and NAD^+ were both 0.7 μM, as measured in separate experiments.

For simplifying the calculations, it was assumed that the maximal oxonol signal was generated by a transient situation of pseudo-equilibrium in which the protonmotive force would be essentially determined by the ambient potential difference between the reducing couple and the oxidizing couple of the NADH:DB reductase reaction. This ambient redox potential (ΔE_m) was calculated considering a standard potential difference of 390 mV as derived from the E_0 value of the couple NAD^+/NADH (−350 mV at pH 8) and that of the DB/DBH_2 couple (40 mV at pH 8). Moreover, it was assumed that the stoichiometry of complex I is of two protons per electron (*1, 4-6, 22, 23*) and that the total protonmotive force equals the electric membrane potential $\Delta\psi$ because of the presence of nigericin in the medium. Given these assumptions, the theoretical $\Delta\psi$ generated by a given ambient redox potential could be calculated by using the following equation(s).

$$-nF\Delta E_m = 2nF\Delta\psi \quad (1)$$

By incorporating the Nernst equation into Eq. 1 with $n=2$ for two electrons are transferred, resulting in $RT/nF=$ 29.5 mV, we obtain:

$$\Delta\psi = -0.5 \times [390 - 29.5\mathrm{Log}([NAD^+]/[NADH] \times [DBH_2]/[DB])] \quad (2)$$

where the $\Delta\psi$ values are expressed in mV. For example, with a 1 : 1 ratio between NAD^+ and NADH, Eq. 2 becomes:

$$\Delta\psi = -0.5 \times [390 - 29.5\mathrm{Log}(100.7/99.3 \times 0.7/29.3)] = -219 \text{ (mV)}.$$

Although these calculations are based upon assumptions which can only approximate the ideal situation of a thermodynamic equilibrium, they yield estimates of $\Delta\psi$ which are in close agreement with the maximal values of the total protonmotive force measured in submitochondrial particles [−220 mV on average (*24, 38*)]. Moreover, the optical signals during reverse-electron transport to NAD^+ promoted by ATP hydrolysis, a reaction close to thermodynamic equilibrium (*22*), were quantitatively similar to the maximal values measured in the forward reaction to Q. We thus consider the theoretical values of $\Delta\psi$ obtained with Eq. 2 to be a reasonable estimate of the maximal membrane potentials generated physiologically by complex I.

RESULTS AND DISCUSSION

Comparison of Different Probes for the $\Delta\psi$ Generated by Complex I—Ideally, a potential-sensitive dye should not inhibit the transport system under investigation and its signal should suffer minimal interference from substrates or internal chromophores of the biological preparation (*18, 20*). In the case of complex I, the first of these requirements is difficult to be met, since so many hydrophobic substances with suitable electrochromic properties inhibit its electron transport activity (*10, 20, 25-28*).

To study the $\Delta\psi$ generated by Complex I, we have initially tested a representative dye of each of the class of carbocyanines, safranines, and oxonols, which are the indicators of membrane potential most frequently used in intracellular organelles and mitochondria (*9, 18, 20, 26*). As reported previously for other dyes of the carbocyanine class (*26-28*), diO-C_5-(3) (3,3'-dipentyloxacarbocyanine iodide or D-272) inhibits complex I, with an average I_{50} of 1.5 μM for the NADH:UBQ reductase activity. Hence, carbocyanine dyes are not suitable for measuring the energy-conserving function of complex I.

Safranine-O, which has been previously used to study the bioenergetic function of complex I (*5, 6*), also inhibits the NADH:UBQ reductase activity in submitochondrial particles, but less potently than carbocyanine dyes (I_{50} = 17 μM). Despite this inhibitory action, safranine can still be used to monitor the membrane potential generated by complex I in coupled ETP_H, as shown in Fig. 1A, *cf.* Ref. *17*. The optical spectrum of safranine undergoes a small blue-shift upon energizing submitochondrial particles with respiratory substrates and the changes of absorbance are maximal at the wavelength couple 511-541 nm, with values that do not exceed 0.01 *A* using NADH (Fig. 1A). Besides this low sensitivity, the optical changes of safranine suffer of a substantial interference by NADH absorbance (Fig. 1A) and respond only to membrane potentials ranging from 20 to *ca.* 90 mV, as verified by calibrations with potassium diffusion potentials (*cf.* Ref. *17*). Owing to these problems, we have discontinued the use of safranine in subsequent experiments.

To assess the $\Delta\psi$ generated by complex I, we have also monitored the oxidation of cytochrome *b* induced by the membrane potential consequent to NADH oxidation (Fig. 1B). In submitochondrial particles reduced with succinate and treated with inhibitors that block both sites of electron communication between cytochrome *b* and Q, namely antimycin A and MOA-stilbene (*29*), the generation of a positive-inside membrane potential induces partial oxidation of the high-potential *b* haem by the low-potential *b* haem (*17, 21, 30*). A transient deflection in the absorbance at 563-575 nm occurs when NADH is added to particles inhibited by complex III inhibitors (Fig. 1B). This deflection, which is synchronous to the absorbance changes of the dyes (Fig. 1), indicates an oxidation of the high-potential *b* haem in response to a transmembrane electric potential built up by complex I. In our experiments, the addition of NADH allows only a few redox turnovers of complex I reducing endogenous Q, since re-oxidation of reduced Q is blocked by complex III inhibitors (addition of the complex

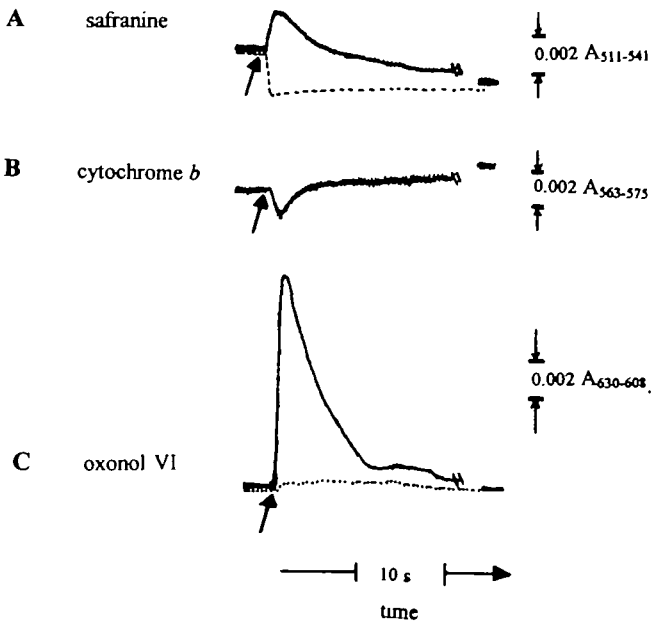

Fig. 1. **Detection of the membrane potential generated by NADH oxidation.** The black arrow indicates the addition of 70 μM NADH after the particles were treated with both antimycin A and MOA-stilbene. In A and B the ETP_H concentration was 1 mg/ml, whilst in C it was 0.17 mg/ml. In A safranine was added to a final concentration of 16 μM, whereas in C oxonol concentration was 2.1 μM. No dye was added in the experiment of trace B, in which cytochrome *b* was previously reduced by 5 mM succinate before the addition of complex III inhibitors. The sensitivity was approximately the same in all experimental traces, which were obtained in the sucrose-tricine buffer supplemented with 2 μM (A and B) or 0.8 μM (C) nigericin. The dashed trace in A was obtained in the presence of 1 μM valinomycin and the dotted trace in C in the presence of 1 μM FCCP. Parallel experiments obtained with faster time resolution of the traces indicated that the half-time of the absorbance changes were very similar in A, B, and C. The final level of the absorbance changes are shown by the separate lines on the right side of the traces.

TABLE I. **The oxonol signals of the non-steady-state and steady-state activity of complex I.** The optical changes of oxonol (2.6-3 μM) in the controls were obtained in the presence of 20 μM carboxin and 0.5-1 μM nigericin; other conditions as in the legend of Fig. 7. The concentrations of rotenone and rolliniastatin-2 inhibited by over 95% the initial rates of the NADH:UBQ reductase activity in the same experiments.

Experiment and addition	Extent of the non-steady-state activity (% control)	Extent of the steady-state activity (% control)
Exp. a (0.2 mg/ml ETP_H)		
None	0.028 *A* (83.8%)	0.077 *A* (93.6%)
20 μM carboxin	0.034 *A* (100%)	0.082 *A* (100%)
0.5 μM valinomycin	−0.003 *A* (0%)	0.010 *A* (12.2%)
1 μg/ml gramicidin	−0.002 *A* (0%)	0.004 *A* (4.8%)
1 μM CCCP	0.000 (0%)	0.000 (0%)
0.1% Tween-20	−0.003 *A* (0%)	0 (0%)
Exp. b (0.4 mg/ml ETP_H)		
None	0.073 *A* (100%)	0.108 *A* (100%)
Rotenone 0.42 nmol/mg	0.020 *A* (27.0%)	0.015 *A* (14.2%)
Rolliniastatin-2 0.3 nmol/mg	0.019 *A* (26.3%)	0.004 *A* (3.7%)
Exp. c (0.17 mg/ml ETP_H)		
None	0.022 *A* (100%)	0.067 *A* (100%)
Rotenone 0.28 nmol/mg	0.006 *A* (27.3%)	0.005 *A* (7.5%)
Rolliniastatin-2 0.23 nmol/mg	0.005 *A* (22.7%)	0.002 *A* (3.0%)

II inhibitor carboxin has also little effect on the membrane potential signal, Table I). Hence, the transient oxidation of cytochrome *b* which is concomitant to the uncoupler-sensitive signals of the dyes (Fig. 1) indicates that a few redox turnovers of complex I produce a significant electrogenic reaction across the membrane, which parallels the non-steady-state proton pumping recorded previously with a pH-sensitive probe (*4*).

Characterization of the Oxonol Response to the $\Delta\psi$ Generated by Complex I—The optical changes of oxonol VI are far greater than those of either safranine or cytochrome *b* when NADH is added to coupled ETP_H (Fig. 1). In the experiment of Fig. 1 the absorbance changes of oxonol are measured at the wavelength couple 630-608 nm as recommended by Bashford and Smith (*18*). However, the red-shift in the optical spectrum of oxonol VI shows an isosbestic point at 601 nm (Fig. 2A). In view of these spectral characteristics, the absorbance changes of oxonol VI are about 30% larger at 630-601 nm than at 630-608 nm (Fig. 2). By considering this and also that during the NADH:Q reductase assay there is no significant spectral interference from the *a* cytochromes, we have routinely measured the oxonol signal at the wavelength couple 630-601 nm (*12*). Figure 2B shows a typical trace at this wavelength couple; the sharp transient generated by the addition of NADH is followed by a larger signal upon addition of the Q substrate initiating the steady-state activity of complex I. The transient signals generated by NADH addition alone are referred to as the non-steady-state activity of complex I (*cf.* Ref. *4*).

The magnitude of the optical changes of oxonol VI depends on the dye-to-membrane ratio as for any other potential-sensitive dye (*18, 20, 26*). A concentration of 0.15 mg/ml ETP_H, as routinely used earlier (*12*), gives the maximal signals with an oxonol concentration of 16-20 nmol per mg of protein, *i.e.* 2.5-3 μM (Fig. 3A). These dye concentrations allow a saturation of both the initial rates of

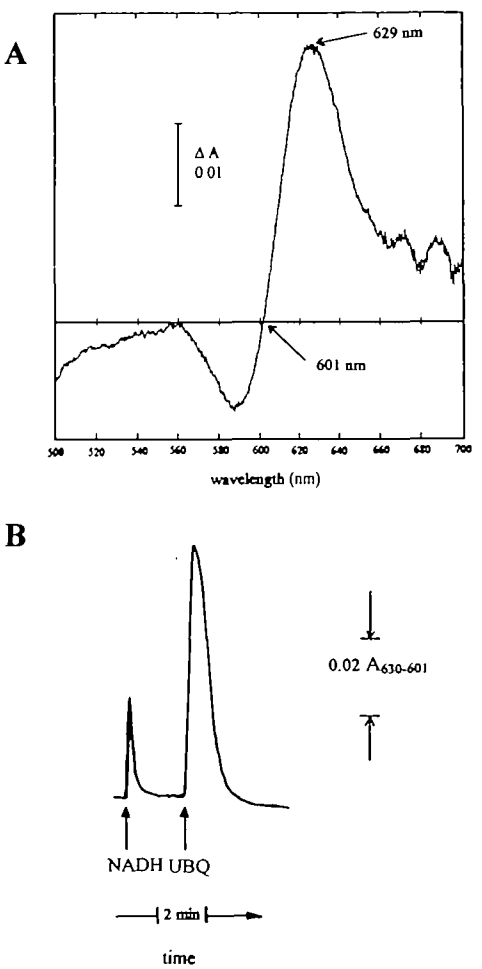

Fig. 2. **Absorbance changes of oxonol VI in ETP_H.** A: Difference spectrum of oxonol VI in energized ETP_H, which were treated with oligomycin and complex III inhibitors and diluted in the sucrose-tricine buffer at 0.18 mg/ml with 2.8 μM oxonol VI. The difference spectrum was obtained from the spectrum of particles energized with both 150 μM NADH and 5 mM succinate *minus* that of particles without substrates. The spectra were performed in a JASCO 7850 spectrophotometer. B: Time-course of the absorbance changes of 2.6 μM oxonol VI with 0.15 mg/ml ETP_H assayed in the sucrose-tricine buffer containing 0.5 μM nigericin. NADH concentration was 150 μM and that of UBQ 30 μM.

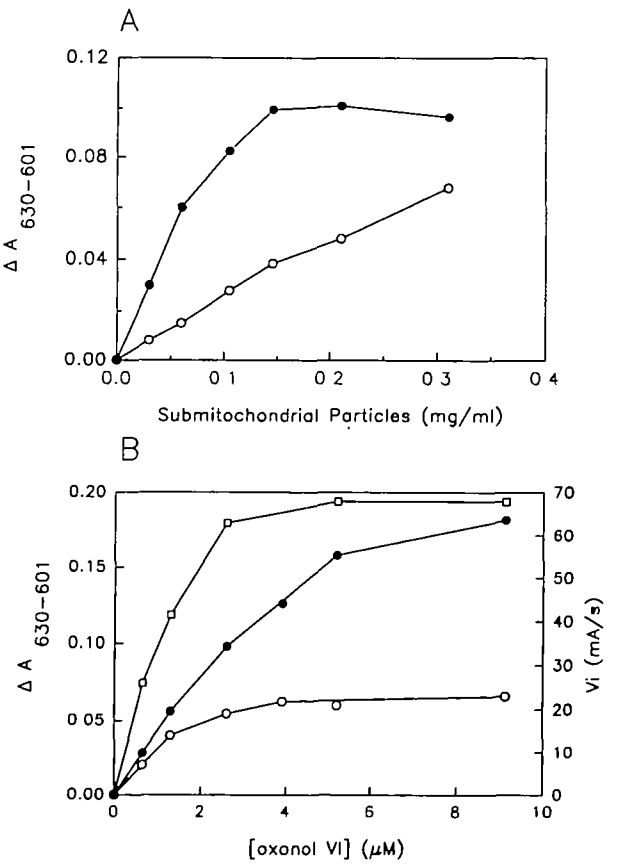

Fig. 3. **Optimization of the signals of oxonol VI.** ETP_H treated with the inhibitors were first reduced by 150 μM NADH for measuring the signal of the non-steady-state activity of complex I; subsequently, 30 μM UBQ was added to stimulate the steady-state activity, as shown in Fig. 2B. A: Extents of the absorbance changes of oxonol VI (3 μM) at different ETP_H concentrations with 1 μM nigericin (○ for the non-steady-state signals and ● for the steady-state signals). B: Extents of the absorbance changes (○ for the non-steady-state signals and ● for the steady-state signals) and initial rates at steady-state (□, ordinate scale on the right of the plot) by increasing concentrations of oxonol VI at a fixed concentration of 0.15 mg/ml ETP_H.

the steady-state activity of complex I and the extents of its non-steady-state activity (Fig. 3B). The extents of the non-steady-state activity are already maximal with oxonol-to-protein ratios around 10 nmol per mg protein (Fig. 3A and Table I), but the saturation point for the extents of the steady-state activity of complex I is at ratios exceeding 60 nmol per mg of protein (*e.g.* 10 μM oxonol in Fig. 3B). Presumably, these high concentrations induce also a substantial non-specific binding of the dye to the membrane (see also Ref. *31*), which is also indicated by the increased proportion of the valinomycin-insensitive signal by increasing the oxonol ratio above 25 nmol per mg of protein (results not shown). However, it is noteworthy that oxonol VI does not inhibit significantly the NADH:Q reductase activity of ETP_H even at concentrations well above 10 μM.

Effect of Ionophores and Inhibitors on the Oxonol Signals by Complex I—As already mentioned, the optical changes of oxonol VI in ETP_H are sensitive to the ionophore valinomycin, which collapses the $\Delta\psi$ component of the protonmotive force (*32, 33*). Normally, the signal promoted by the steady-state activity of NADH:Q reductase is over 80% sensitive to valinomycin, whilst the signal promoted by the addition of NADH under non-steady state conditions is abolished by valinomycin (Table I). Protonophores such as CCCP and gramicidin, and also detergents, abolish all the oxonol signals promoted by complex I activity (Fig. 1 and Table I).

The inhibitory effect of specific inhibitors of complex I such as rotenone and rolliniastatin-2 tends to be more potent for the steady-state activity than for the non-steady-state activity of complex I (Table I). In particular, inhibitor concentrations that reduce the steady-state reductase activity by over 95% still allow oxonol signals which are 20–30% of the control signals (Table I and results not shown). It can be assumed that complex I works in single turnover in the presence of a saturating inhibitor such as rotenone and the oxonol signals recorded under such conditions approach one-fourth of those obtained in the absence of inhibitors (Table I). This observation suggests that non-inhibited complex I may produce four turnovers under non-steady state conditions. Such a deduction was confirmed by measurements with high concentration of particles (0.5–1 mg/ml) to enable direct detection of NADH oxidation above the background. By considering a complex I content of 0.04 nmol per mg of protein (*16*), the level of NADH rapidly oxidized by mitochondrial particles was generally around four molecules per molecule of enzyme (results not shown). The NADH dependence of the oxonol signal, moreover, indicated that the membrane potential generated under non-steady-state conditions requires much less electron input than that generated by the NADH:Q reductase activity.

Nigericin specifically collapses the ΔpH component of the protonmotive force and is thus expected to enhance the absorbance changes of oxonol (*7, 18, 32, 33*). Some stimulation of the oxonol absorbance changes promoted by the NADH:Q reductase activity occurs at concentrations of nigericin which completely collapse the ΔpH of the particles [*i.e.* 0.2 μM (*32*)]. However, concentrations of nigericin exceeding 1 μM most frequently decrease the amplitude of the oxonol signals (Fig. 4). A surfactant-like property of the ionophore is likely to be responsible for its inhibitory effects at high concentrations (*33*).

The oxonol signals produced by the ubiquinol oxidase activity are less sensitive to high concentration of nigericin than the signals generated by the NADH:Q reductase activity under the same conditions (Fig. 4). Since nigericin does not inhibit the redox activity of complex I (data not shown), the enhanced sensitivity to nigericin of the oxonol signals generated by NADH oxidation might reflect a different contribution of the $\Delta\psi$ component in the protonmotive force produced by complex I and complex III (*34*). This is in agreement with early results obtained with equilibrium dialysis methods which indicated that the contribution of electric potential to the total protonmotive force is different in NADH respiration than in succinate respiration (*24*).

Calibration of the Oxonol Signals with the Membrane Potential—We have calibrated the oxonol signals with several approaches. The classical calibration with diffusion potentials using KCl (*19, 31, 35*) indicates that oxonol has a threshold response around −50 mV and its optical signals increase non-linearly with the imposed potential (Fig. 5). However, the absorbance changes of the dye approach 0.04 *A* for the maximal potentials achieved with potassium diffusion (around −160 mV, circle symbols in Fig. 5), whereas much larger signals are usually observed for the steady-state activity of complex I (Figs. 2B and 3 and Table I, *cf.* Ref. *12*).

To obtain an evaluation of the oxonol responses that encompasses the range of physiological potentials, we have performed experiments in which the maximal activity of the NADH:Q reductase was varied in response to different ambient redox potentials. The assumption is that the maximal oxonol signals associated with the NADH:Q reductase activity respond to a pseudo-equilibrium situation in which the protonmotive force is essentially equivalent to the free energy released by the redox reaction, which can be varied by changing the ambient redox potential with different ratios of the electron donor and/or acceptor couple (see "MATERIALS AND METHODS," *cf.* Ref. 7). The theoretical $\Delta\psi$ values thus obtained with Eq. 2 range between

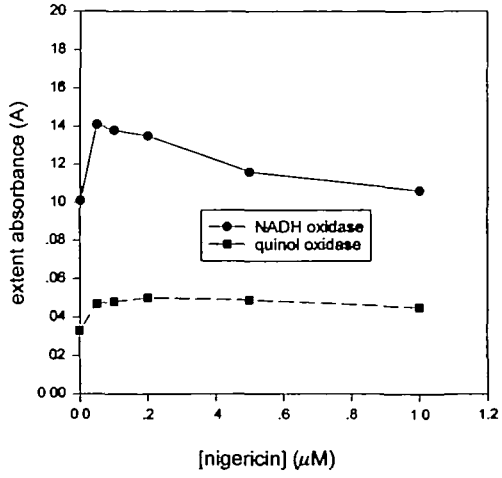

Fig. 4. **Effect of nigericin on the oxonol signals generated by complex I.** Conditions were the same as those of Fig. 2B except for the concentration of NADH, which was 97 μM, and for the absence of complex III inhibitors, to measure the signals generated by the oxidation of NADH (filled circles) and DBH_2 (33 μM, filled squares).

−178 and −246 mV and the corresponding oxonol signals are reported in Fig. 5 (square symbols). There is a sharp dependence of the optical changes to potentials between −160 and −200 mV, and saturation of the dye response for theoretical $\Delta\psi$ values above −200 mV (Fig. 5). Consequently, the dependence of the oxonol signals upon the combination of diffusion potentials and theoretical potentials has a sigmoidal shape, with −50 and −220 mV as the approximate limits (Fig. 5).

The signals of oxonol VI that we usually measure are higher than those reported earlier (*7-9*), presumably because our experimental protocol maximizes the intensity of the dye response. Nevertheless, the optical changes obtained here in the NADH oxidase activity of well-coupled ETP_H (represented by the black bar on the right of Fig. 5) fall within the upper limit of the oxonol signal of the NADH:Q reductase (Fig. 5). This suggests that complex I may produce a membrane potential equivalent to the maximal protonmotive force that can be measured in submitochondrial particles [about −220 mV (*24, 35*)]. The apparent saturation of the oxonol signals for theoretical $\Delta\psi$ values around −220 mV could simply depend on the natural limits of the mitochondrial protonmotive force. However, as for other potential-sensitive dyes, the nonlinear calibration of oxonol VI also derives from factors intrinsic to its response mechanism, such as absorption on the membrane surface (*7-9, 19*), interference by surface potentials (*31*), and saturation of the binding to the membrane (*8*).

The Initial Rate versus the Time-Course of the Oxonol Signals at Steady-State—For a rigorous evaluation of the membrane potential of complex I it is necessary to measure also the initial rate of the oxonol signals (*5, 6, 12*). When rapid mixing apparata are not available for an accurate determination of the initial rates, the alternative is to quantitate the entire time-course of the absorbance changes. In our previous studies on the quinone specificity of the NADH:Q reductase we have quantitated the absorbance changes of oxonol VI by a graphical approximation of the time-course (*12, 13*). The transient signal of the dye can be approximated to a triangle having the maximal extent of absorbance as its height and the half-time of the decay to the baseline as its width. This transformation formally corresponds to a rate, for it is expressed in absorbance units per second, and generally correlates well with the initial rates of the absorbance changes (Fig. 6 and Ref. *12*). The correlation is essentially linear for a wide range of conditions, preparations and substrates (Fig. 6). The linearity of this correspondence remains also in preparations less tightly-coupled than those of the data in Fig. 6, but the slope of the correlation decreases significantly.

Clear deviations from the linear correlation between the triangular transformation of the time-course and the initial rates occur when the rates exceed 150 mA/s, due in part to the limitations of our rapid mixing apparatus, and with effectors that alter the membrane integrity. With pure complex I inhibitors such as rolliniastatin-2, the decrease in the maximal extent of the oxonol signal is always associated with a decrease in the rate of its decay, so that the width of the transient is larger and the overall time-course is flatter

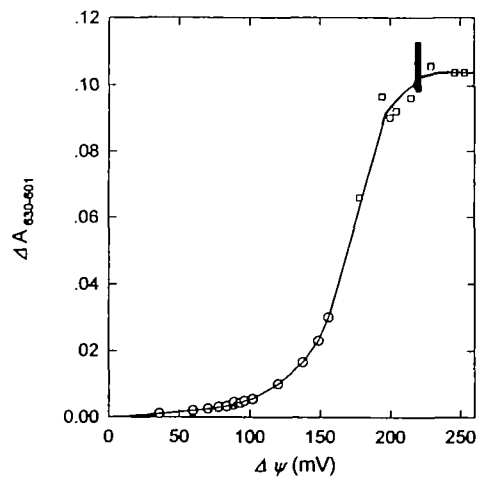

Fig. 5. **Calibrations of oxonol signals with membrane potentials.** The extents of the absorbance changes of 3 μM oxonol were measured with 0.15 mg/ml ETP_H pre-equilibrated with the sucrose-tricine buffer containing 1 mM KCl in the presence of 2 μM valinomycin. The symbols ○ represent the oxonol signals measured by imposing potassium diffusion potentials with a constant ionic strength of either 40 or 400 mM (for the highest potentials). The symbols □ represent the oxonol signals measured by manipulating thermodynamically the NADH:DB reductase reaction with the assumptions and conditions described under "MATERIALS AND METHODS." The values of $\Delta\psi$ are theoretically estimated using Eq. 2 and could be considered the maximal values that complex I may produce physiologically. The black bar on the top right corresponds to the range of signals (with an average of 0.106 ± 0.006 *A*) of nine different experiments of NADH oxidation with 0.1 mM NADH in the presence of 0.5-1 μM nigericin (*cf.* Ref. *12*). These optical changes are correlated with a $\Delta\psi$ value of −220 mV, which corresponds to the average value of the maximal protonmotive force measured in submitochondrial particles (*24*).

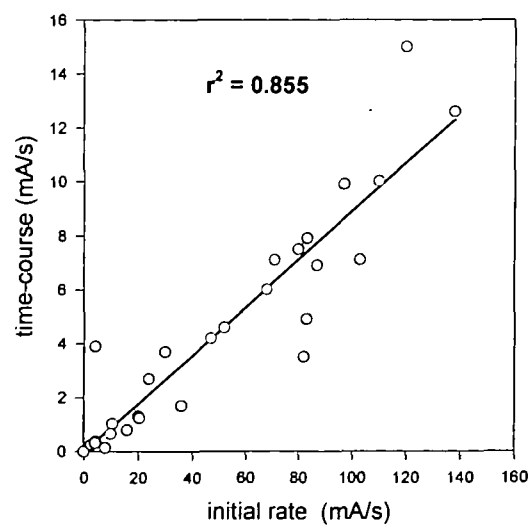

Fig. 6. **Correlation between initial rate and time-course of the oxonol signals.** The oxonol signals were obtained in different preparations of tightly-coupled ETP_H using either the NADH:Q reductase reaction (with both UBQ and DB as the substrates) or the ubiquinol oxidase reaction (with either $UBQH_2$ or DBH_2 as the substrates), in the absence or the presence of various concentrations of pure respiratory inhibitors such as rolliniastatin-2 and MOA-stilbene. The time-courses were elaborated according to the triangular approximation described in the text.

than the control (*cf.* Fig. 7A). By contrast capsaicin, a well-known inhibitor of complex I (*36*), also uncouples the mitochondrial membrane, most likely because of its acid-base properties. The time-courses of the oxonol signals in the presence of capsaicin are sharper than those obtained with a pure complex I inhibitor, since the decay time is similar to that of the control signal (Fig. 7 and results not shown). To demonstrate the uncoupling action of capsaicin, Fig. 7C shows the comparison of the potency on the NADH: Q reductase activity of complex I with that on the membrane potential generated by the hydrolytic activity of ATP-synthase. The inhibition on this membrane potential is not due to inhibition of the ATPase activity, which is insensitive to capsaicin at the concentrations used (results not shown).

The quantitative interpretation of the oxonol signals could facilitate the screening of new compounds developed as mitochondrial inhibitors, for instance pesticides of potential agrochemical application (*37*). In this view, it is noteworthy that the oxonol assay can be applied to submitochondrial particles from a variety of sources, even if signals comparable to those measured in beef heart are obtained only with sheep and donkey preparations (M. Degli Esposti, A. Ngo, and A. Ghelli, unpublished data).

Evaluation of the Charge Separation Produced by Complex I—An alternative approach to evaluate quantitatively the responses of oxonol VI is to compare the non-steady-state reactions of complex III with those of complex I. For this we have used a ETP_H preparation containing little endogenous cytochrome *c*, which allows the measure-

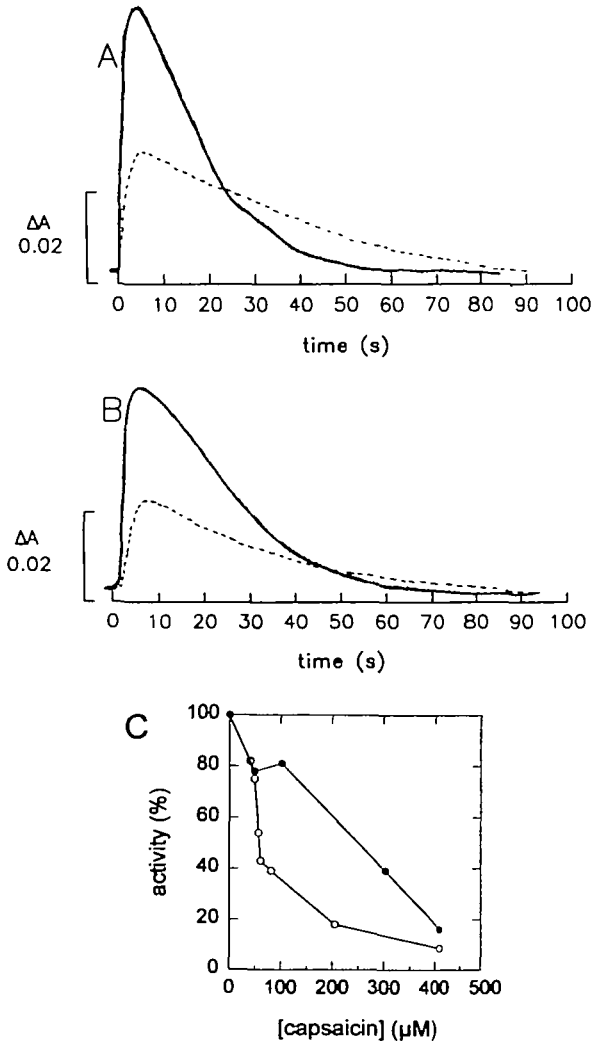

Fig. 7. **Effect of inhibitors on the time-course of the oxonol signals.** ETP_H (0.15 mg/ml) were assayed in the presence of 3 μM oxonol and 1 μM nigericin with 100 μM NADH and 30 μM UBQ. The traces initiate with the addition of UBQ. A: The solid and dotted line indicate the oxonol signals in the absence and presence of 15 nM of rolliniastatin-2, respectively. B: The solid and dotted line indicate the oxonol signals in the absence and presence of 80 μM capsaicin, respectively. C: The reductase activity of complex I (○) was measured as reported previously (*12*) and the initial rates of oxonol signals generated by the hydrolysis of 1 mM ATP (●) were measured in ETP_H which were not previously treated with oligomycin.

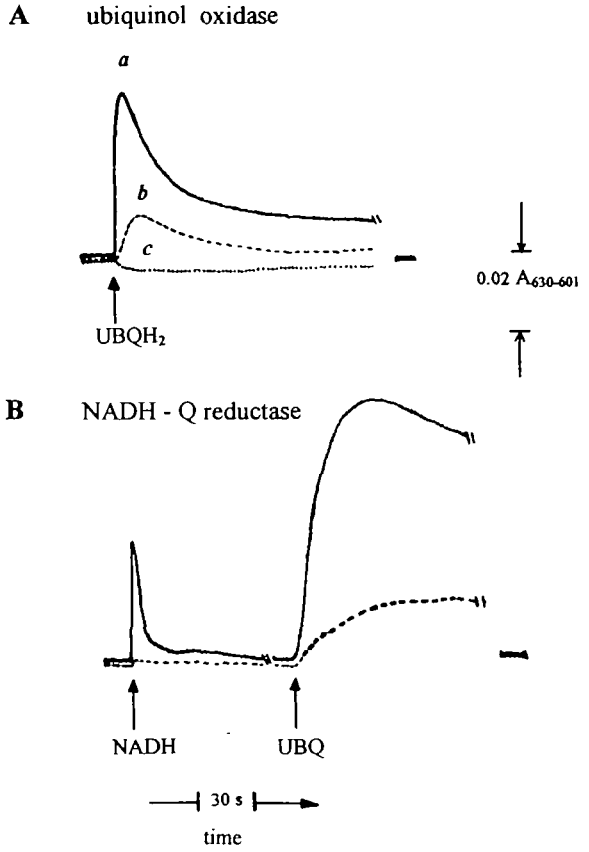

Fig. 8. **Comparison of the oxonol signals generated by complex III and complex I.** Cytochrome *c*-depleted ETP_H (0.15 mg/ml) were assayed with 2.7 μM oxonol VI. The medium did not contain nigericin, so that the oxonol traces purely reflected the electric membrane potential generated by the respiratory complexes. A: Traces promoted by the ubiquinol oxidase activity of the particles. The rates of NADH and ubiquinol oxidase activity were much slower than normal due to the low content of cytochrome *c*. The concentration of $UBQH_2$ was 25 μM. Trace *a* was obtained without complex III inhibitors, trace *b* with particles pre-treated with 1 nmol/mg of antimycin A, and trace *c* with particles that had been treated with both antimycin A and 3 nmol/mg of MOA-stilbene. B: The same particles treated with both complex III inhibitors as in A were used to measure the oxonol traces promoted by the activity of complex I with 76 μM NADH and 26 μM UBQ. The dashed trace was obtained in the presence of 1 μM valinomycin. The final level of absorbance is shown by the separate line on the right of the traces.

ment of the oxonol signals associated with a few turnovers of complex III. Addition of reduced UBQ ($UBQH_2$) to these particles produces a transient signal of *ca.* 0.04 *A*, most of which decreases rapidly—the subsequent slow return to the baseline is due to the limited ubiquinol oxidase activity *via* the residual cytochrome *c* (Fig. 8). The addition of a saturating concentration of antimycin reduces by two-thirds the oxonol signal promoted by $UBQH_2$ (trace b in Fig. 8A) and the addition of the other complex III inhibitor MOA-stilbene eliminates the signal completely (trace c in Fig. 8A). The oxonol signal in the presence of antimycin reflects the single-turnover of quinol oxidation at center "o" in the Q-cycle (*38-40*) that generates membrane potential essentially through the electron transport between the two haems of cytochrome *b* (*30, 38-40*). Since these haems are separated by about 2 nm along the membrane normal (*29, 39*), the antimycin-insensitive reaction of ubiquinol oxidation promotes an electrogenic separation of about 0.4 net charge across the membrane width (*38, 40*).

In the presence of both antimycin and MOA-stilbene, the addition of NADH promotes a transient signal of *ca.* 0.03 *A* (Fig. 8B), which is quantitatively similar to the antimycin-sensitive signal generated by complex III. Hence, the non-steady-state activity of complex I produces an electrogenic reaction equivalent to the separation of approximately 0.6 net charge across the width of the membrane. The antimycin-sensitive electrogenic reaction in complex III (Fig. 8) results from the transport of electrons from the high-potential *b* haem embedded in the membrane to a bound Q that is reduced at the negative face of the membrane with uptake of scalar protons (*38, 40*). Spatial arrangement of the redox groups in the crystal structure of bovine complex III (*41*) is consistent with these deductions originally based on electrogenic measurements (*17, 38, 40*). How can we explain a similar electrogenic reaction in complex I?

The Electrogenic Processes in Complex I—The oxonol signals generated by electrons transferred through the cofactors of the complex to endogenous Q fall within a well-defined region of the calibrated response of oxonol, corresponding to $\Delta\psi$ values which are generally between −130 and −180 mV (Figs. 2B and 3A; *cf.* Fig. 5). In view of the quantitative similarity of this membrane potential to that generated by the antimycin-sensitive reduction of Q in complex III (Fig. 8), the established Q-cycle mechanism of complex III could guide the interpretation of the electrogenic processes associated with Q reduction in complex I.

Based on analogies with the Q-cycle mechanism, recent schemes postulate that complex I produces charge separation during the transport of electrons between different forms of bound Q located at the opposite sides of the membrane (*42-45*) and by electrogenic movements of protons through pumps or channels (*1, 4, 43-45*). That nigericin has little effect on the membrane potential built up by a few turnovers of complex I (Fig. 4A) suggests that movements of protons by complex I might also compensate the charge separation consequent to electron transport within the low-dielectric membrane domain (*46*). Yet the $\Delta\psi$ signals produced by few turnovers of complex I are abolished by valinomycin (Fig. 8 and Table I) and thus derive from non-compensated movements of electrons across the membrane.

An attractive possibility is that complex I contains a membrane-embedded cofactor which transfers electrons to Q at the negative side of the membrane, similarly to the high-potential *b* haem of complex III. Weiss *et al.* (*23*) first postulated that an internal Q site may fulfill this role and facilitates electron transport to the iron-sulfur cluster N2, which was earlier proposed to be located in the membrane (*2, 23*). This latter proposal is now in conflict with the

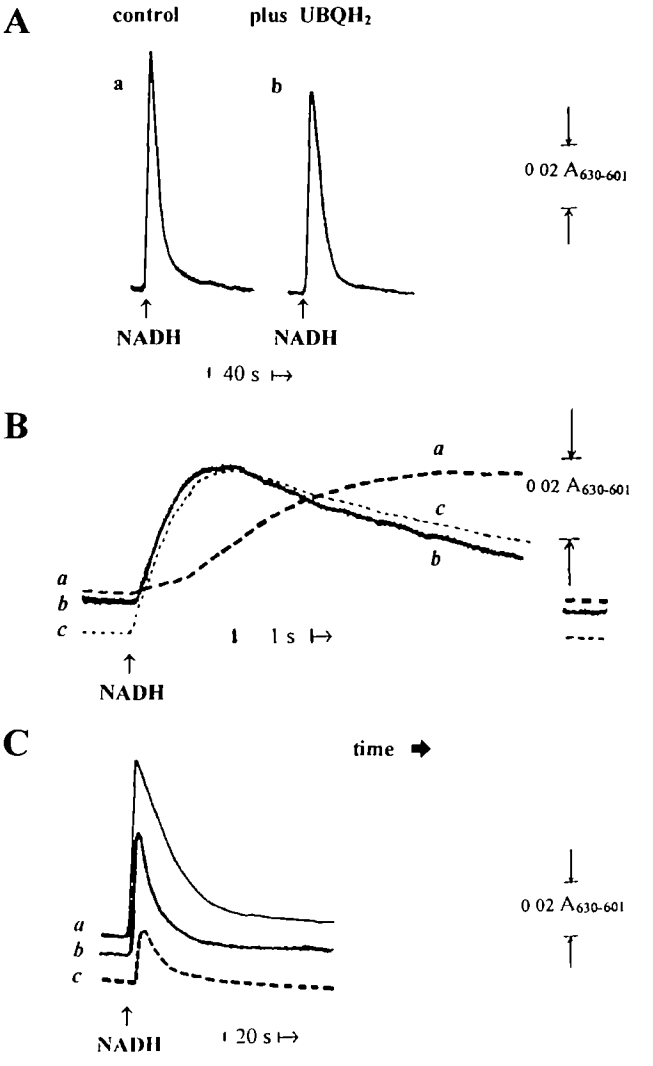

Fig. 9. **The electrogenic reactions of complex I under limited turnover.** The concentration of oxonol was 2.4-2.6 μM in all experiments. A: 0.3 mg/ml of ETP_H were treated with complex III inhibitors and activated by 100 μM NADH in the absence of nigericin. a, control; b, in the presence of 20 μM reduced UBQ. B: Time-resolved kinetics of the non-steady-state signals obtained with 100 μM NADH and 0.2 mg/ml of ETP_H treated with complex III inhibitors and oligomycin in the presence of 25 μM carboxin and 0.5 μM nigericin. Trace *a* (long-dashed line) was obtained in the presence of 20 μM DBH_2; trace *b* (solid line) had no additions (control), and trace *c* (short-dashed line) was obtained in the presence of 200 μM K-ferricyanide. Note that the time scale is 40-fold larger than in A. C: Overall signals obtained in a different preparation under the same conditions as in B except that the concentration of carboxin was 20 μM (which still allowed about 20% of complex II activity). Trace *a* was obtained after the addition of 100 μM K-ferricyanide to oxidize the particles, whereas trace *b* is the control without additions before NADH. Trace *c* was recorded after equilibration with 1 mM succinate to reduce endogenous Q; similar results were obtained with an equimolar ratio of succinate to fumarate in the absence of carboxin.

structural information on the subunits that could bind the N2 cluster, which are most likely located at the periphery of the membrane (*1, 3, 4, 43-45*). In the absence of any firm evidence for a membrane cofactor other than Q in complex I, variations of the concept of an internal Q site have now been incorporated in several proposals which focus on the protonmotive function of bound semiquinones (*1, 3, 4, 42-45*). Indeed, a semiquinone radical is associated with complex I and involved in energy conservation for it is sensitive to uncouplers (*42, 47-49*).

Recent models for complex I mechanism postulate also a fundamental role for ubiquinol reversebly bound to the enzyme (*43-45*). The influence of ubiquinol in the electrogenic reactions of the complex is easily tested by measuring the oxonol signals after manipulation of the redox state of the pool of endogenous Q, as shown in Fig. 9. The increased concentration of endogenous ubiquinol induced by either succinate reduction or by addition of exogenous quinols effectively decreases the rate, and also the amplitude of the oxonol signals (Fig. 9). This contradicts any prediction that ubiquinol could be essential to promote the electrogenic reactions of complex I. Conversely, full oxidation of the Q pool by ferricyanide has little effect on the $\Delta\psi$ produced by complex I, and generally enhances the extents of the signals (Fig. 9 and results not shown). This further indicates that pre-formed ubiquinol could not be essential for the protonmotive function of complex I.

Conclusion and Perspectives—In conclusion, the oxonol measurements described here constitute a valuable tool for: (i) the study of the bioenergetic function of complex I at steady-state; (ii) the analysis of the protonmotive reactions of complex I under conditions of limited turnover. In perspective, by monitoring the optical signals of oxonol in the presence of specific inhibitors it will be possible to follow also pre-steady-state reactions of complex I. These measurements will have the dual advantage of requiring limited quantities of biological material and producing relatively slow rates of reaction. For instance, the absorbance changes of oxonol generated by the addition of 0.1 mM NADH to 0.1 mg/ml of tightly-coupled particles has an half time of 200 ms. By considering that the concentration of reacting complex I in the particles is rate determining with excess of NADH, this 200 ms half-time compares well with the half-time of a few ms obtained in experiments of rapid quenching low-temperature EPR, which used 20-30 mg/ml of submitochondrial particles (*49, 50*). Because the minimal mixing time of rapid quenching techniques is around 5 ms, the time resolution of key steps in the electron transport of complex I has not been achieved so far (*49-51*). Hence, the kinetic analysis of the optical changes of oxonol-VI could offer a convenient tool for evaluating internal steps of the electron transport from NADH to Q and monitor at the same time the protonmotive reactions of complex I.

We thank H. McLennan, A. Ngo, and M. Ratta for their help to some experiments and M. Crimi, G. Venturoli, P. Turina, L. Helfenbaum, B.A. Melandri, and U. Brandt for helpful discussions.

REFERENCES

1. Walker, J. (1992) The NADH:ubiquinone oxidoreductase (complex I) of respiratory chains. *Q. Rev. Biophys.* **25**, 253-324
2. Ohnishi, T. (1993) NADH-quinone oxidoreductase, the most complex complex. *J. Bioenerg. Biomembr.* **25**, 325-329
3. Friedrich, T., Steinmuller, K., and Weiss, H. (1995) The proton-pumping respiratory complex I of bacteria and mitochondria and its homologue in chloroplasts. *FEBS Lett.* **367**, 107-111
4. Degli Esposti, M. and Ghelli, A. (1994) The mechanism of proton and electron transport in mitochondrial complex I. *Biochim. Biophys. Acta* **1187**, 116-120
5. Di Virgilio, F. and Azzone, G.F. (1982) Activation of site I redox-driven H^+ pump by exogenous quinones in intact mitochondria. *J. Biol. Chem.* **257**, 4106-4113
6. Wikström, M. (1984) Two protons are pumped from the mitochondrial matrix per electron transferred between NADH and ubiquinone. *FEBS Lett.* **169**, 300-304
7. Bashford, C.L. and Thayer, W.S. (1977) Thermodynamics of the electrochemical proton gradient in bovine heart submitochondrial particles. *J. Biol. Chem.* **252**, 8459-8463
8. Smith, J.C. and Chance, B. (1979) Kinetics of the potential-sensitive extrinsic probe oxonol VI in beef heart submitochondrial particles. *J. Membr. Biol.* **46**, 255-282
9. Smith, J.C. (1990) Potential-sensitive molecular probes in membranes of bioenergetic relevance. *Biochim. Biophys. Acta* **1016**, 1-28
10. Ahmed, I. and Krishnamoorthy, G. (1994) Anomalous response of oxonol-V to membrane potential in mitochondrial proton pumps. *Biochim. Biophys. Acta* **1188**, 131-138
11. Hayashi, M., Miyoshi, T., Sato, M., and Unemoto, T. (1992) Properties of respiratory chain-linked Na^+-independent NADH-quinone reductase in a marine *Vibrio alginolyticus*. *Biochim. Biophys. Acta* **1099**, 145-151
12. Degli Esposti, M., Ngo, A., McMullen, G., Ghelli, A., Sparla, F., Benelli, B., Ratta, M., and Linnane, A.W. (1996) The specificity of mitochondrial complex I for ubiquinones. *Biochem. J.* **313**, 327-334
13. Degli Esposti, M., Ngo, A., Ghelli, A., Benelli, B., Carelli, V., McLennan, H., and Linnane, A.W. (1996) The interaction of Q analogs, particularly hydroxydecyl benzoquinone (idebenone), with the respiratory complexes of heart mitochondria. *Arch. Biochem. Biophys.* **330**, 395-400
14. Hansen, M. and Smith, A.L. (1964) Studies on the mechanism of oxidative phosphorylation. VII. Preparation of a submitochondrial particle (ETP_H) which is capable of fully coupled oxidative phosphorylation. *Biochim. Biophys. Acta* **81**, 214-222
15. Ghelli, A. (1994) Ph.D. thesis, University of Bologna, Bologna
16. Degli Esposti, M., Ghelli, A., Ratta, M., Cortes, D., and Estornell, E. (1994) Natural substances (acetogenins) from the family *Annonaceae* are powerful inhibitors of mitochondrial NADH dehydrogenase (Complex I). *Biochem. J.* **301**, 161-167
17. Gopher, A. and Gutman, M. (1980) The effect of membrane potential on the redox state of cytochrome b_{561} in antimycin-inhibited submitochondrial particles. *J. Bioenerg. Biomembr.* **12**, 349-367
18. Bashford, C.L. and Smith, J.C. (1979) The use of optical probes to monitor membrane potential in *Methods in Enzymology* (Fleischer, S. and Packer, L., eds.) Vol. 55, pp. 569-582, Academic Press, New York
19. Rottenberg, H. (1989) Proton electrochemical potential gradient in vesicles, organelles and prokaryotic cells in *Methods in Enzymology* (Fleischer, S. and Fleischer, B., eds.) Vol. 172, pp. 63-84, Academic Press, New York
20. Freedman, J.C. and Novak, T.S. (1989) Optical measurement of membrane potential in cells, organelles, and vesicles in *Methods in Enzymology* (Fleischer, S. and Fleischer, B., eds.) Vol. 172, pp. 102-122, Academic Press, New York
21. Bechmann, G. and Weiss, H. (1991) Regulation of the proton/electron stoichiometry of mitochondrial ubiquinol:cytochrome *c* reductase by membrane potential. *Eur. J. Biochem.* **195**, 431-438
22. Rottenberg, H. and Gutman, M. (1977) Control of the rate of reverse electron transport in submitochondrial particles by the free energy. *Biochemistry* **16**, 3220-3227
23. Weiss, H., Friedrich, T., Hofhaus, G., and Preis, D. (1991) The respiratory-chain NADH dehydrogenase (complex I) of mito-

chondria. *Eur. J. Biochem.* **197**, 563-576
24. Sorgato, C.M. and Ferguson, S.J. (1979) Variable proton conductance of submitochondrial particles. *Biochemistry* **18**, 5737-5742
25. Sayre, L.M., Singh, M.P., Arora, P.K., Wang, F., McPeak, R.J., and Hoppel, C.L. (1990) Inhibition of mitochondrial respiration by analogues of the dopaminergic neurotoxin 1-methyl-4-phenylpyridinium: structural requirements for accumulation-dependent enhanced inhibitory potency on intact mitochondria. *Arch. Biochem. Biophys.* **280**, 274-283
26. Waggoner, A.S. (1979) Dye indicators of membrane potential. *Annu. Rev. Biophys. Bioeng.* **8**, 47-68
27. Ahmed, I. and Krishnamoorthy, G. (1994) Probing of coenzyme quinone binding site of mitochondrial NADH:CoQ reductase by fluorescence dynamics. *Biochemistry* **33**, 9675-9683
28. Anderson, W.M., Wood, J.M., and Anderson, A.C. (1993) Inhibition of mitochondrial and *Paracoccus denitrificans* NADH-ubiquinone reductase by oxycarbocyanine dyes. *Biochem. Pharmacol.* **45**, 2115-2122
29. Degli Esposti, M., DeVries, S., Crimi, M., Ghelli, A., Patarnello, T., and Meyer, A. (1993) Mitochondrial cytochrome *b*: evolution and structure of the protein. *Biochim. Biophys. Acta* **1143**, 243-271
30. Miki, T., Miki, M., and Orii, Y. (1994) Membrane potential-linked reversed electron transfer in the beef heart cytochrome bc_1 complex reconstituted into potassium-loaded phospholipid vesicles. *J. Biol. Chem.* **269**, 1827-1833
31. Beeler, T.J., Farmen, R.H., and Martonosi, A.N. (1981) The mechanism of voltage-sensitive dye responses on sarcoplasmic reticulum. *J. Membr. Biol.* **62**, 113-117
32. Rottenberg, H. and Moreno-Sanchez, R. (1993) The proton pumping activity of H^+-ATPases: an improved fluorescence assay. *Biochim. Biophys. Acta* **1183**, 161-170
33. Reed, P.W. (1979) Ionophores in *Methods in Enzymology* (Fleischer, S. and Packer, L., eds.) Vol. 55, pp. 435-454, Academic Press, New York
34. Helfenbaum, L., Ngo, A., Ghelli, A., Linnane, A.W., and Degli Esposti, M. (1997) Proton pumping of mitochondrial complex I: differential activation by analogs of ubiquinone. *J. Bioenerg. Biomembr.* (in press)
35. Nicholls, D.G. and Ferguson, S.J. (1992) *Bioenergetics 2*, Academic Press, London
36. Yagi, T. (1990) Inhibition by capsaicin of NADH-quinone oxidoreductases is correlated with the presence of energy-coupling site 1 in various organisms. *Arch. Biochem. Biophys.* **281**, 305-311
37. Jewess, P.J. (1994) Insecticides and acaricides which act at the rotenone-binding site of mitochondrial NADH:ubiquinone oxidoreductase; competitive displacement studies using a ^{3}H-labelled rotenone analogue. *Biochem. Soc. Trans.* **22**, 247-251
38. Glaser, E.G. and Crofts, A.R. (1984) A new electrogenic step in the ubiquinol:cytochrome c_2 oxidoreductase complex of *Rhodopseudomonas sphaeroides*. *Biochim. Biophys. Acta* **766**, 322-333
39. Trumpower, B.L. (1990) The protonmotive Q cycle. *J. Biol. Chem.* **265**, 11409-11412
40. Robertson, D.E. and Dutton, P.L. (1988) The nature and magnitude of the charge-separation reactions of the ubiquinol cytochrome c_2 oxidoreductase. *Biochim. Biophys. Acta* **935**, 273-291
41. Yu, C.-A., Xia, J.-X., Kachurin, A.M., Yu, L., Xia, D., Kim, H. and Deisenhofer, J. (1996) Crystallization and preliminary structure of beef heart mitochondrial cytochrome-bc_1 complex. *Biochim. Biophys. Acta* **1275**, 47-53
42. Vinogradov, A.D. (1993) Kinetics, control, and mechanism of ubiquinone reduction by the mammalian respiratory chain-linked NADH-ubiquinone reductase. *J. Bioenerg. Biomembr.* **25**, 367-375
43. Sled, V.D., Burbaev, D.S., Grivennikova, V.G., Moroz, I.A., Vinogradov, A.D., and Ohnishi, T. (1996) Bound forms of ubiquinone and mechanism of $\Delta\mu H^+$ generation in complex I. *9th EBEC Short Reports*, p. 149
44. Ohnishi, T. (1996) Oral presentation at the *9th EBECmeeting*. Louvain-la-Nueve, Belgium, August 1996
45. Brandt, U. (1997) Proton-translocation by membrane-bound NADH:Ubiquinone-oxidoreductase (Complex I) through redox-gated ligand conduction. *Biochim. Biophys. Acta* **1318**, 79-91
46. Rich, P.R. (1996) Electron transfer complexes coupled to ion translocation in *Protein Electron Transfer* (Bendall, D.S., ed) pp. 217-248, BIOS Scientific Publisher, Oxford
47. Kotlyar, A.B, Sled, V.D., Burbaev, D.S., Moroz, I.A., and Vinogradov, A.D. (1990) Coupling site I and the rotenone-sensitive ubisemiquinone in tightly coupled submitochondrial particles. *FEBS Lett.* **264**, 17-20
48. Vinogradov, A.D., Sled, V.D., Burbaev, D.S., Grivennikova, V.G., Motoz, I.A., and Ohnishi, T. (1995) Energy-dependent Complex I-associated ubisemiquinones in submitochondrial particles. *FEBS Lett.* **370**, 83-87
49. De Jong, A.M., Kotlyar, A.B., and Albracht, S.P.J. (1994) Energy-induced structural changes in NADH:Q oxidoreductase of the mitochondrial respiratory chain. *Biochim. Biophys. Acta* **1186**, 163-171
50. Van Balzen, R. and Albracht, S.P.J. (1989) The pathway of electron transport in NADH:Q oxidoreductase. *Biochim. Biophys. Acta* **974**, 311-320
51. Orme-Johnson, N.R., Hansen, R.H., and Beinert, H. (1974) Electron paramagnetic resonance-detectable electron acceptors in beef heart mitochondria. Reduced diphosphopyridine nucleotide ubiquinone reductase segment of the electron transfer system. *J. Biol. Chem.* **249**, 1922-1927